Published in final edited form as:
Neuroscience. 2010 April 28; 167(1): 135–142. doi:10.1016/j.neuroscience.2010.01.056.

LOSS OF SYNAPTOTAGMIN IV RESULTS IN A REDUCTION IN SYNAPTIC VESICLES AND A DISTORTION OF THE GOLGI STRUCTURE IN CULTURED HIPPOCAMPAL NEURONS

C. P. ARTHUR[a,b], **C. DEAN**[c], **M. PAGRATIS**[a], **E. R. CHAPMAN**[c], and **M. H. B. STOWELL**[a,*]

[a]MCD Biology, University of Colorado, Boulder, CO, 80309, USA

[b]The Scripps Research Institute, Department of Cell Biology, La Jolla, CA, 92037, USA

[c]Howard Hughes Medical Institute, Department of Physiology, University of Wisconsin, Madison, WI, 53706, USA

Abstract

Fusion of synaptic vesicles with the plasma membrane is mediated by the SNARE (soluble NSF attachment receptor) proteins and is regulated by synaptotagmin (syt). There are at least 17 syt isoforms that have the potential to act as modulators of membrane fusion events. Synaptotagmin IV (syt IV) is particularly interesting; it is an immediate early gene that is regulated by seizures and certain classes of drugs, and, in humans, syt IV maps to a region of chromosome 18 associated with schizophrenia and bipolar disease. Syt IV has recently been found to localize to dense core vesicles in hippocampal neurons, where it regulates neurotrophin release. Here we have examined the ultrastructure of cultured hippocampal neurons from wild-type and syt IV −/− mice using electron tomography. Perhaps surprisingly, we observed a potential synaptic vesicle transport defect in syt IV −/− neurons, with the accumulation of large numbers of small clear vesicles (putative axonal transport vesicles) near the trans-Golgi network. We also found an interaction between syt IV and KIF1A, a kinesin known to be involved in vesicle trafficking to the synapse. Finally, we found that syt IV −/− synapses exhibited reduced numbers of synaptic vesicles and a twofold reduction in the proportion of docked vesicles compared to wild-type. The proportion of docked vesicles in syt IV −/− boutons was further reduced, 5-fold, following depolarization.

Keywords

synaptotagmin IV; Golgi; synapse; tomography; hippocampus

Fusion of synaptic vesicles with the plasma membrane is mediated by the SNARE (soluble NSF attachment receptor) complex of proteins and syt I (Chapman, 2002; Koh and Bellen, 2003). During depolarization, calcium binds to the C2 domains of syt I, inducing a strong binding interaction between syt I, SNARE proteins, and the phospholipids of the target membrane (Chicka et al., 2008). This promotes the formation of a fusion pore through which neurotransmitter is released (Bai et al., 2004; Tucker et al., 2004; Zhang et al., 2002). The interaction of syt I with target membrane phospholipids is essential for membrane fusion, and the calcium sensitivity and kinetics of phospholipid binding varies among the remaining 16 syt isoforms (Bhalla et al., 2005; Chicka et al., 2008; Hui et al., 2005).

*Correspondence to: M. H. B. Stowell, MCD Biology, University of Colorado, Boulder, CO, 80309, USA. Tel: +1-303-735-2983. michael.stowell@colorado.edu (M. H. B. Stowell)..

Syt IV was originally identified as an immediate early gene that is upregulated following neuronal depolarization (Vician et al., 1995) and maps to a region of human chromosome 18 associated with schizophrenia and bipolar disease (Ferguson et al., 2001). Syt IV has a number of very interesting characteristics: it is developmentally regulated (Berton et al., 2000; Ibata et al., 2000), upregulated by seizures (Tocco et al., 1996; Vician et al., 1995), regulated by psychoactive drugs (Denovan-Wright et al., 1998; Ferguson et al., 2001; Peng et al., 2002), and induced by neuronal activity (Ibata et al., 2000). One of the C2 domains of syt IV harbors an aspartic acid to serine substitution that is conserved in human, *Drosophila melanogaster*, *C. elegans*, mouse, and rat (Ferguson et al., 2000). Syt-IV is unable to bind phospholipids (Chapman et al., 1998) rendering it potentially unable to promote calcium-dependent fusion.

It was recently reported that syt IV is localized to neurotrophin-containing vesicles in hippocampal neurons, where it inhibits the release of BDNF to affect synaptic function and plasticity (Dean et al., 2009). Syt IV also affects a number of vesicle recycling properties in peptidergic nerve terminals in the posterior pituitary (Zhang et al., 2009). Interestingly syt IV also appears to play a role in the maturation of secretory granules in neuroendocrine cells (Ahras et al., 2006; Eaton et al., 2000) suggesting that it may also function in the movement of vesicles.

Although syt IV knockout mice were generated a number of years ago (Ferguson et al., 2000), an ultrastructural analysis of synapses in these mice is lacking. Here, using electron tomography of cultured hippocampal neurons from wild-type and syt IV −/− mice we found that a loss of syt IV results in a structural defect in the Golgi that is associated with a dramatic increase in the trans-Golgi network size and the accumulation of what appear to be large numbers of small clear vesicles, possibly axonal transport vesicles, in the cell body. Concomitantly, there is a decrease in the total number of synaptic vesicles, as well as the proportion of docked vesicles in presynaptic terminals, compared to wild-type synapses. Upon KCl depolarization this number of docked vesicles decreases further in knockout synapses as compared to wild-type. Together these data suggest that syt IV plays a role both in the Golgi and in the maintenance of normal numbers of synaptic vesicles in presynaptic terminals.

EXPERIMENTAL PROCEDURES

Hippocampal neuron culture

Hippocampi were isolated from P1–3 mice, as described previously (Banker and Cowan, 1977; Brewer et al., 1993) in accordance with the guidelines of the National Institutes of Health, as approved by the Animal Care and Use Committee of the University of Wisconsin, Madison. Hippocampi were treated with trypsin for 20 min at 37 °C, and triturated to dissociate cells. Cells were plated at 25,000–50,000 cells/cm^2 on 12 mm coverslips (Carolina Biologicals, Burlington, NC, USA) that had been coated with poly-lysine for 30 min. Neurons were cultured in Neurobasal medium supplemented with 2% B-27 and 2 mM Glutamax (Gibco/Invitrogen, Carlsbad, CA, USA). Syt IV knockout mice were provided by H. Herschman. Antibodies used are as follows: Synaptotagmin IV, vesicular GABA transporter (VGAT), Synaptophysin (Synaptic Systems, Göttingen, Germany), golgi matrix protein 130 KD (GM130), Synaptotagmin I, KIF1A, and myosin I (Santa Cruz Biotechnology, Santa Cruz, CA, USA), VGlut1 (Millipore, Billerica, MA, USA).

Confocal fluorescence microscopy

Cultured neurons from syt IV knockout and wild-type littermates were fixed with 4% paraformaldehyde in 100 mM sodium phosphate buffer, permeabilized and blocked with

phosphate-buffered saline containing 10% goat serum and 0.1% Triton X-100 and labeled with anti-GM130 and anti-synaptophysin antibodies. For Fig. 2, neurons were labeled with anti-VGluT1 and anti-VGAT. Cells were then visualized using a Zeiss LSM 510 laser confocal microscope at a magnification of 60×. Images were analyzed using the ImageJ software package (Irving et al., 2007). Twenty-two fluorescence images each of labeled Golgi from wild-type and syt IV −/− neurons were thresholded at a common value and volumetric data were calculated. For Fig. 2c, nine images from three different cultures were analyzed using Metamorph software (Improvision). VGluT and VGAT channels were thresholded separately to include all recognizable puncta, and average intensity was determined. Statistical significance was determined by a Student's *t*-test where * $P<0.05$, ** $P<0.01$, and *** $P<0.001$.

Electron microscopy

Three mm copper electron microscopy grids were prepared with two coats of Formvar by placing grids on top of a Formvar film floating on water and then retrieving them onto a 12 mm coverslip, to which the grids adhered. Grids on coverslips were then plasma glow discharged to make them hydrophilic, polylysine coated overnight at 37 °C, and then coated with laminin for 2–3 h. Coverslips were UV treated, and hippocampal neurons, as prepared above, were plated at a density of 50–100,000 cells/cm^2. 10–15 DIV neurons were rapidly frozen under high pressure in a BAL-TEC HPM-010 high-pressure freezer (Technotrade International, Manchester, NH). Frozen cells were freeze substituted into acetone containing 2% osmium tetroxide and 0.1% uranyl acetate at −80 °C and then slowly warmed to room temperature. After substitution and warming, cells were embedded in EPON-Araldite. 250 nm thick sections of embedded cells were cut and stained using 2% uranyl acetate and lead citrate, and 15 nm gold particles laid on top of the sample as fiducials for tomographic reconstruction. Imaging was performed using a Tecnai F20 (FEI, Eindhoven, The Netherlands) operated at 200 kV and a magnification of 25,000×. Grids of serial sections were place in a high-tilt stage and the sample was tilted from 60° to −60° at 1° increments along a single axis relative to the axis of the TEM beam. A total of 120 images with a pixel size of 0.91 nm were collected via a charge coupled device (CCD) camera (Gatan, 2048×2048 pixels). The sample was then rotated 90° about the z-axis and imaging was again performed through ±60°. Images were processed and a tomographic reconstruction generated using the ETOMO software package (The Boulder Laboratory for 3-D Electron Microscopy of Cells). Tomograms were modeled using the IMOD software program (The Boulder Laboratory for 3-D Electron Microscopy of Cells). Surface renderings were performed by hand tracing the membrane of every other section of the reconstruction, then meshing contours to give a precise rendering of the three-dimensional information. Vesicles were rendered by predicting the spherical nature of the vesicle surface and then contouring accordingly. Samples to be stimulated were treated with 90 mM KCl for 90 s prior to freezing. Number of samples imaged are as follows: wild-type unstimulated (20 boutons from 10 separate cultures), wild-type stimulated (17 boutons from eight separate cultures), syt IV −/− unstimulated (18 boutons from eight separate cultures), syt IV −/− stimulated (15 boutons from eight separate cultures).

Immunoprecipitations

Mouse brains were homogenized in 4 mM HEPES (pH 7.4), 0.32 M sucrose, and 1 mM EDTA, with protease inhibitors. Cells were pelleted by centrifugation and solubilized with 20 mM Tris (pH 8.0), 140 mM NaCl, 10% glycerol, 1% TX-100, and 2 mM EDTA. Antibodies used are as follows: Synaptotagmin IV, Synaptotagmin I (Synaptic Systems, Göttingen, Germany), Kif1A (Santa Cruz Biotechnology, Santa Cruz, CA, USA). Insoluble material was removed by centrifugation, and the soluble extract was incubated with the respective antibodies (α-Syt IV, α-Syt I, α-Kif1A) bound to protein A-sepharose. After

incubation overnight at 4 °C, beads were washed with homogenization buffer and bound proteins were analyzed using SDS-PAGE and immunoblotting.

RESULTS

Loss of syt IV results in a profound decrease in both the total number of synaptic vesicles and the proportion of active zone docked vesicles

To examine the ultrastructural consequences of syt IV's absence from synapses we performed EM tomography on syt IV −/− and wild-type littermate neuron cultures. Electron tomographic reconstructions of cultured hippocampal neurons showed a dramatic decrease in the total number of synaptic vesicles in syt IV −/− compared to wild-type terminals under both resting conditions and following strong stimulation to induce vesicle recycling (90 mM KCl for 90 s) (Fig. 1a, and quantified in b, c). Confocal microscopy also revealed a significant reduction in the fluorescence intensity of synaptic vesicle proteins at syt IV −/− synapses compared to wild-type (Fig. 2c). This decrease in vesicle number may be due to syt IV −/− vesicles being more fusogenic than wild-type, a decrease in endocytosis, or a deficit in synaptic vesicle biogenesis. We found that, while the total number of vesicles decreased to approximately 35% of wild-type in the absence of syt IV, upon stimulation the total number of vesicles decreased even more, to approximately 24% of wild-type (Fig. 1b). Investigation of the number of vesicles docked in the active zone showed a reduction in docked vesicles in syt IV −/− synapses, to 53% of wild-type. Following stimulation, even fewer vesicles were docked in syt IV −/− boutons (18% of wild-type) (Fig. 1c). These data suggest that synaptic vesicles in syt IV knockout terminals are more likely to fuse in response to stimulation than wild-type vesicles, which could cause the observed reduction in synaptic vesicle number. However, it remains possible that syt IV might also play a role, directly or indirectly, in synaptic vesicle biogenesis and/or endocytosis, in addition. A defect in endocytosis seems unlikely, however, given that loss of syt IV favored rapid endocytosis in the posterior pituitary (Zhang et al., 2009).

Syt IV knockout neurons have an extended, irregularly shaped Golgi

The decrease in the number of synaptic vesicles present at syt IV −/− synapses raises the question as to whether or not synaptic vesicle precursors are being produced and delivered normally to the synapse. Previous work (Yonekawa et al., 1998) reported that removal of the kinesin KIF1A results in a similar loss of synaptic vesicles as well as a dramatic structural defect in the Golgi. Accordingly, we examined the Golgi morphology and ultrastructure in syt IV −/− and wild-type neurons using laser confocal fluorescence microscopy. In cells stained with the Golgi marker GM130 we observed a ~33% enlargement of the Golgi in syt IV −/− neurons as compared to wild-type (Fig. 2a, d). The same wild-type and syt IV −/− neurons were then examined using EM tomography and the total volume of the modeled Golgi area was calculated. Similar to the fluorescence data, the Golgi in syt IV −/− cells showed a ~40% increase in overall volume as compared with wild-type (Fig. 2b–d).

Syt IV knock out neurons exhibit a large pool of small clear vesicles adjacent to the trans-Golgi network

A pool of vesicles in close proximity to the Golgi was observed in KIF1A −/− neurons, with no such vesicle pool present in wild-type neurons (Yonekawa et al., 1998). Syt IV −/− neurons studied here displayed a similar phenotype. In contrast to wild-type neurons they contained a large (>1×0.2×0.5 μm^3) pool of vesicles in close proximity (<1.0 μm) to the TGN (Fig. 3a). Closer inspection revealed that the majority of “juxtaGolgi” vesicles in syt IV −/− cells were small clear vesicles and only a small number were clathrin-coated (~70 out 395) (Fig. 3b–d). The trafficking of synaptic proteins from the Golgi has been reported to occur via bundles of small clear vesicles intermixed with large dense-core vesicles

(LDCVs) (Tao-Cheng, 2007). The observation of the TGN vesicle pools in syt IV −/− neurons suggests that syt IV plays an active role in vesicle transport and/or vesicle maturation from the TGN.

Syt IV co-immunoprecipitates with the kinesin KIF1A

Given the similarity between the KIF1A −/− and Syt IV −/− phenotypes, we used immunoprecipitation to determine if these proteins associate with each other. Mouse brain detergent extracts were incubated with α-KIF1A, α-syt IV, or α-syt I antibodies and subsequently precipitated using protein A Sepharose beads (Sigma). Immunoprecipitates were denatured and analyzed by SDS-PAGE and immunoblotting (Fig. 4). Syt IV was immunoprecipitated using α-KIF1A antibodies, and the same was true for KIF1A using α-syt IV. KIF1A was also pulled down by syt I. However, syt I and syt IV did not co-immunoprecipitate each other to an appreciable extent. Protein A Sepharose beads alone yielded no detectable syt IV, KIF1A, or syt I. These data reveal a potential interaction, which may be direct or indirect, between KIF1A and syt IV and is consistent with previous yeast two-hybrid studies (Park et al., 2005).

DISCUSSION

Previous studies of syt IV have found it to be potentially involved in a wide variety of activities in the brain. Syt IV has been shown to localize to the Golgi (Ibata et al., 2000), and to neurotrophin-containing vesicles in both axons and dendrites where it regulates BDNF release (Dean et al., 2009). It is upregulated in response to seizures (Tocco et al., 1996; Vician et al., 1995), and interestingly syt IV mRNA was increased in the song circuit of zebra finches during singing (Poopatanapong et al., 2006). Syt IV has been found to promote biogenesis and maturation of secretory granules in neuroendocrine cells, and has been reported to mediate glutamate release in astrocytes (Zhang et al., 2004). Given the high levels of syt IV in the pituitary, where it affects several aspects of vesicle fusion (Zhang et al., 2009), it may also be involved in neuropeptide secretion.

In hippocampal neurons, syt I acts as the main calcium sensor in neurotransmitter release, while syt IV acts to negatively regulate neurotrophin release (Dean et al., 2009). In Drosophila post-synaptic syt IV at the NMJ (Adolfsen et al., 2004) acts in a retrograde manner to enhance presynaptic function (Yoshihara et al., 2005). Unlike the mammalian isoform, Drosophila syt IV retains its ability to bind phospholipids (Littleton et al., 1999; Dai et al., 2004) and thus may positively regulate exocytosis, while mammalian syt IV is a negative regulator of exocytosis.

The removal of syt IV in mice appears to have no gross phenotypic characteristics. The mice present normally with no seizures but have reduced anxiety and depression compared with wild-type mice (Ferguson et al., 2004) and show deficiencies in learning and memory associated with the hippocampus (Ferguson et al., 2000). In the current study we have extended the examination of syt IV removal in mice by imaging cultured hippocampal neurons in three-dimensions, using electron tomography and confocal fluorescence microscopy. We found a dramatic decrease in the number of synaptic vesicles by electron tomography, thus demonstrating a presynaptic effect of the loss of syt IV. That this depletion of synaptic vesicles at the hippocampal synapse does not translate into an alteration in basal synaptic transmission may suggest possible functions for syt IV. The decrease in vesicle number we observe may be due to syt IV −/− synaptic vesicles being more fusogenic than wild-type vesicles. If syt IV −/− synaptic vesicles are more fusogenic, it is possible that when syt IV is not present, terminals need fewer vesicles for normal basal transmission, and fewer presynaptic axonal transport vesicles containing synaptic proteins

are transported to synapses. This could result in the observed decrease in synaptic vesicles in syt IV −/− presynaptic terminals and accumulation of vesicles near the Golgi.

We observed a significant reduction in synaptic vesicle protein immunostaining fluorescence intensity in syt IV −/− synapses, compared to wild-type synapses. However, this reduction was much less dramatic than the reduction in synaptic vesicle number in syt IV −/− boutons observed by EM tomography. It is thus possible that synaptic vesicles are present near synapses (within the 200–300 μm resolution limit of light microscopy) in syt-IV knockouts, but are farther from the active zone than in wild-type synapses, resulting in a dramatic difference in vesicle number specifically at active zones. Another possibility is that synaptic vesicle proteins are present at higher amounts in the plasma membrane in syt-IV knockout neurons, compared to wild-type, which may be a possible consequence of increased vesicle exocytosis. A third (less likely) possibility is that synaptic vesicles of syt-IV knockout neurons contain higher proportions of synaptic vesicle proteins than wild-type synaptic vesicles.

Twenty-five to thirty synaptic vesicles are thought to actively recycle during maximal stimulation at hippocampal synapses (Harata et al., 2001). At least two distinct pools of vesicles exist at these synapses, one active during low frequency stimulation which releases vesicles faster, and one utilized during high frequency stimulation which shows slower release kinetics and is released after the faster releasing pool (Vanden Berghe and Klingauf, 2006). It is possible that syt IV −/− synapses contain a pool of vesicles required for basal function, and are missing a separate pool of vesicles, which require syt IV for their trafficking. A similar depletion of synaptic vesicles has been seen with the loss of other synaptic proteins. Synapsin knockouts have reduced numbers of synaptic vesicles in resting conditions (Rosahl et al., 1995) but unlike syt IV knockouts (Ferguson et al., 2004) show decreases in other vesicle proteins, suggesting a mis-localization of synaptic proteins in syt IV knockouts. Synapsin knockouts have normal LTP (Rosahl et al., 1995) suggesting that synapses can function normally during long-term potentiation with reduced vesicle numbers. Syt IV knockouts exhibit increased LTP (Dean et al., 2009), despite the reduction in SV number we observe by EM tomography.

Recent work has found that syt IV acts as a negative regulator of neutrophin secretion, which reduces presynaptic vesicle fusion (Dean et al., 2009). This observation leads to another possible interpretation of our results: a loss of syt IV would lead to increased neurotrophin release and a subsequent increase in synaptic vesicle fusion and an overall decrease in the synaptic vesicle pool at synaptic boutons, rather tha a long-range defect in trafficking of synaptic vesicle proteins to synapses from the Golgi.

Syt IV's function most likely extends further than effects on vesicle fusion and recycling. The appearance of an irregularly shaped Golgi in syt IV −/− neurons suggests that the Golgi is more than a reservoir of syt IV. In addition, the large pool of small clear vesicles in close proximity to the TGN observed in neurons lacking syt IV, suggests that syt IV may affect maturation of vesicles in hippocampal neurons as it does in neuroendocrine cells (Ahras et al., 2006; Eaton et al., 2000). Syt IV may also affect trafficking of vesicles from the Golgi to distal sites, either pre- or post-synaptically. Indeed, we have detected an interaction between syt IV and KIF1A, a kinesin known to associate with both synaptic vesicles and neurotrophin-containing vesicles (Park et al., 2005). The phenotype we observe in syt IV −/− neurons is similar to the phenotype previously reported for KIF1A knockout mice: a loss of synaptic vesicles and accumulation of unknown vesicles near the TGN. Future work is needed to determine whether there is a trafficking defect in neurons lacking syt IV. In addition, future studies are needed to precisely define the function of syt IV in maintaining Golgi structure.

Abbreviation

SNARE soluble NSF attachment receptor

REFERENCES

Adolfsen B, Saraswati S, Yoshihara M, Littleton JT. Synaptotagmins are trafficked to distinct subcellular domains including the postsynaptic compartment. J Cell Biol. 2004; 166:249–260. [PubMed: 15263020]

Ahras M, Otto GP, Tooze SA. Synaptotagmin IV is necessary for the maturation of secretory granules in PC12 cells. J Cell Biol. 2006; 173:241–251. [PubMed: 16618809]

Bai J, Wang CT, Richards DA, Jackson MB, Chapman ER. Fusion pore dynamics are regulated by synaptotagmin*t-SNARE interactions. Neuron. 2004; 41:929–942. [PubMed: 15046725]

Banker GA, Cowan WM. Rat hippocampal neurons in dispersed cell culture. Brain Res. 1977; 126:397–342. [PubMed: 861729]

Berton F, Cornet V, Iborra C, Garrido J, Dargent B, Fukuda M, Seagar M, Marqueze B. Synaptotagmin I and IV define distinct populations of neuronal transport vesicles. Eur J Neurosci. 2000; 12:1294–1302. [PubMed: 10762358]

Bhalla A, Tucker WC, Chapman ER. Synaptotagmin isoforms couple distinct ranges of Ca2+, Ba2+, and Sr2+ concentration to SNARE-mediated membrane fusion. Mol Biol Cell. 2005; 16:4755–4764. [PubMed: 16093350]

Brewer GJ, Torricelli JR, Evege EK, Price PJ. Optimized survival of hippocampal neurons in B27-supplemented Neurobasal, a new serum-free medium combination. J Neurosci Res. 1993; 35:567–576. [PubMed: 8377226]

Chapman ER. Synaptotagmin: a Ca(2+) sensor that triggers exocytosis? Nat Rev Mol Cell Biol. 2002; 3:498–508. [PubMed: 12094216]

Chapman ER, Desai RC, Davis AF, Tornehl CK. Delineation of the oligomerization, AP-2 binding, and synprint binding region of the C2B domain of synaptotagmin. J Biol Chem. 1998; 273:32966–32972. [PubMed: 9830048]

Chicka MC, Hui E, Liu H, Chapman ER. Synaptotagmin arrests the SNARE complex before triggering fast, efficient membrane fusion in response to Ca2+ Nat Struct Mol Biol. 2008; 15:827–835. [PubMed: 18622390]

Dai H, Shin OH, Machius M, Tomchick DR, Sudhof TC, Rizo J. Structural basis for the evolutionary inactivation of Ca2+ binding to synaptotagmin 4. Nat Struct Mol Biol. 2004; 11:844–849. [PubMed: 15311271]

Dean C, Liu H, Dunning FM, Chang PY, Jackson MB, Chapman ER. Synaptotagmin IV modulates synaptic function and LTP by regulating BDNF release. Nat Neurosci. 2009; 12:767–776. [PubMed: 19448629]

Denovan-Wright EM, Newton RA, Armstrong JN, Babity JM, Robertson HA. Acute administration of cocaine, but not amphetamine, increases the level of synaptotagmin IV mRNA in the dorsal striatum of rat. Brain Res Mol Brain Res. 1998; 55:350–354. [PubMed: 9582453]

Eaton BA, Haugwitz M, Lau D, Moore HP. Biogenesis of regulated exocytotic carriers in neuroendocrine cells. J Neurosci. 2000; 20:7334–7344. [PubMed: 11007891]

Ferguson GD, Anagnostaras SG, Silva AJ, Herschman HR. Deficits in memory and motor performance in synaptotagmin IV mutant mice. Proc Natl Acad Sci U S A. 2000; 97:5598–5603. [PubMed: 10792055]

Ferguson GD, Vician L, Herschman HR. Synaptotagmin IV: biochemistry, genetics, behavior, and possible links to human psychiatric disease. Mol Neurobiol. 2001; 23:173–185. [PubMed: 11817218]

Ferguson GD, Wang H, Herschman HR, Storm DR. Altered hippocampal short-term plasticity and associative memory in synaptotagmin IV (−/−) mice. Hippocampus. 2004; 14:964–974. [PubMed: 15390175]

Harata N, Ryan TA, Smith SJ, Buchanan J, Tsien RW. Visualizing recycling synaptic vesicles in hippocampal neurons by FM 1–43 photoconversion. Proc Natl Acad Sci U S A. 2001; 98:12748–12753. [PubMed: 11675506]

Hui E, Bai J, Wang P, Sugimori M, Llinas RR, Chapman ER. Three distinct kinetic groupings of the synaptotagmin family: candidate sensors for rapid and delayed exocytosis. Proc Natl Acad Sci U S A. 2005; 102:5210–5214. [PubMed: 15793006]

Ibata K, Fukuda M, Hamada T, Kabayama H, Mikoshiba K. Synaptotagmin IV is present at the Golgi and distal parts of neurites. J Neurochem. 2000; 74:518–526. [PubMed: 10646502]

Irving BA, Weltman JY, Brock DW, Davis CK, Gaesser GA, Weltman A. NIH ImageJ and slice-O-Matic computed tomography imaging software to quantify soft tissue. Obesity (Silver Spring). 2007; 15:370–376. [PubMed: 17299110]

Koh TW, Bellen HJ. Synaptotagmin I, a Ca2+ sensor for neurotransmitter release. Trends Neurosci. 2003; 26:413–422. [PubMed: 12900172]

Littleton JT, Serano TL, Rubin GM, Ganetzky B, Chapman ER. Synaptic function modulated by changes in the ratio of synaptotagmin I and IV. Nature. 1999; 400:757–760. [PubMed: 10466723]

Park H-Y, Yea SS, Jang WH, Chung J-Y, Lee SK, Kim S-J, Yang Y-I, Kim J-Y, Park Y-H, Seog D-H. Kinesin superfamily KIF1A protein binds to synaptotagmin XI. Korean J Anat. 2005; 38:403–411.

Peng W, Premkumar A, Mossner R, Fukuda M, Lesch KP, Simantov R. Synaptotagmin I and IV are differentially regulated in the brain by the recreational drug 3,4-methylenedioxymethamphetamine (MDMA). Brain Res Mol Brain Res. 2002; 108:94–101. [PubMed: 12480182]

Poopatanapong A, Teramitsu I, Byun JS, Vician LJ, Herschman HR, White SA. Singing, but not seizure, induces synaptotagmin IV in zebra finch song circuit nuclei. J Neurobiol. 2006; 66:1613–1629. [PubMed: 17058190]

Rosahl TW, Spillane D, Missler M, Herz J, Selig DK, Wolff JR, Hammer RE, Malenka RC, Sudhof TC. Essential functions of synapsins I and II in synaptic vesicle regulation. Nature. 1995; 375:488–493. [PubMed: 7777057]

Tao-Cheng JH. Ultrastructural localization of active zone and synaptic vesicle proteins in a preassembled multi-vesicle transport aggregate. Neuroscience. 2007; 150:575–584. [PubMed: 17977664]

Tocco G, Bi X, Vician L, Lim IK, Herschman H, Baudry M. Two synaptotagmin genes, Syt1 and Syt4, are differentially regulated in adult brain and during postnatal development following kainic acid-induced seizures. Brain Res Mol Brain Res. 1996; 40:229–239. [PubMed: 8872307]

Tucker WC, Weber T, Chapman ER. Reconstitution of Ca2+-regulated membrane fusion by synaptotagmin and SNAREs. Science. 2004; 304:435–438. [PubMed: 15044754]

Vanden Berghe P, Klingauf J. Synaptic vesicles in rat hippocampal boutons recycle to different pools in a use-dependent fashion. J Physiol. 2006; 572:707–720. [PubMed: 16439431]

Vician L, Lim IK, Ferguson G, Tocco G, Baudry M, Herschman HR. Synaptotagmin IV is an immediate early gene induced by depolarization in PC12 cells and in brain. Proc Natl Acad Sci U S A. 1995; 92:2164–2168. [PubMed: 7892240]

Yonekawa Y, Harada A, Okada Y, Funakoshi T, Kanai Y, Takei Y, Terada S, Noda T, Hirokawa N. Defect in synaptic vesicle precursor transport and neuronal cell death in KIF1A motor protein-deficient mice. J Cell Biol. 1998; 141:431–441. [PubMed: 9548721]

Yoshihara M, Adolfsen B, Galle KT, Littleton JT. Retrograde signaling by Syt 4 induces presynaptic release and synapse-specific growth. Science. 2005; 310:858–863. [PubMed: 16272123]

Zhang Q, Fukuda M, Van Bockstaele E, Pascual O, Haydon PG. Synaptotagmin IV regulates glial glutamate release. Proc Natl Acad Sci U S A. 2004; 101:9441–9446. [PubMed: 15197251]

Zhang X, Kim-Miller MJ, Fukuda M, Kowalchyk JA, Martin TF. Ca2+-dependent synaptotagmin binding to SNAP-25 is essential for Ca2+-triggered exocytosis. Neuron. 2002; 34:599–611. [PubMed: 12062043]

Zhang Z, Bhalla A, Dean C, Chapman ER, Jackson MB. Synaptotagmin IV: a multifunctional regulator of peptidergic nerve terminals. Nat Neurosci. 2009; 12:163–171. [PubMed: 19136969]

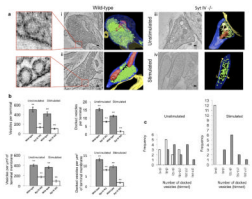

Fig. 1.

Syt IV −/− synapses have a decreased number of vesicles prior to stimulation and a decreased number of docked vesicles following stimulation, compared to WT synapses. All synapse images are from a 10 nm slice in the Z-plane of a tomographic reconstruction from 250 nm thick sections of cultured hippocampal neurons (WT or syt IV −/−). Scale bar in (i), (ii), and (iv) is 60 nm. Scale bar in (iii) is 70 nm. (a) (i) (L–R) WT hippocampal synapse (vesicle number is representative of the wild-type mean (504 vesicles)). Enlarged area to the left shows an example of a docked vesicle. Surface rendering of the full three-dimensional tomographic reconstruction generated using the IMOD software program, where blue indicates presynaptic membrane; yellow, postsynaptic membrane; red, mitochondria; and green, synaptic vesicles. (ii) (L–R) WT hippocampal synapse, stimulated with KCl for 90 s prior to processing for EM (vesicle number is representative of the WT mean (415 vesicles)). Enlarged area to the left shows an example of a docked vesicle. Surface rendering of the full three-dimensional tomographic reconstruction. (iii) (L–R) Syt IV −/− hippocampal synapse (vesicle number is representative of the knockout mean (177 vesicles)). Surface rendering of the full three-dimensional tomographic reconstruction. (iv) (L–R) Syt IV −/− hippocampal synapse, stimulated with KCl for 90 s prior to processing for EM (vesicle number is representative of the knockout mean (102 vesicles)). Surface rendering of the full three-dimensional tomographic reconstruction. (b) (L–R, top to bottom) Comparison of the mean number of vesicles per synaptic terminal, for WT versus syt IV −/−, under resting and stimulated (90 mM KCl, 90 s) conditions. WT mean=504 (resting) and 415 (stimulated) vesicles/terminal. Syt IV −/− mean=177 (resting) and 102 (stimulated) vesicles/terminal. Comparison of the mean number of docked vesicles per synaptic terminal, for WT versus syt IV −/−, under resting and stimulated conditions. WT mean=15 (resting) and 11 (stimulated) vesicles/terminal, syt IV −/− mean=8 (resting) and 2 (stimulated) vesicles/terminal. Comparison of the mean density of vesicles (vesicles/μm^2 of synaptic membrane). WT mean=402 (resting) and 359 (stimulated) vesicles/μm^2. Syt IV −/− mean=172 (resting) and 92 (stimulated) vesicles/μm^2. Comparison of the mean density of docked vesicles (docked vesicles/μm^2 of synaptic membrane). WT mean=13 (resting) and 9.6 (stimulated) vesicles/μm^2. Syt IV −/− mean=7.9 (resting) and 1.8 (stimulated) vesicles/μm^2. Error bars indicate SEM. (c) Comparison of the frequency distribution of the number of docked vesicles between WT (gray bars) and syt IV −/− (white bars) synapses under resting and stimulated conditions. (Number of samples imaged are as follows: WT unstimulated (20 boutons from 10 separate cultures), WT stimulated (17 boutons from eight separate cultures), syt IV −/− unstimulated (18 boutons from eight separate cultures), syt IV −/− stimulated (15 boutons from eight separate cultures; error bars indicate SEM; statistical significance was determined by a Student's *t*-test where * $P<0.05$, ** $P<0.01$, and *** $P<0.001$).

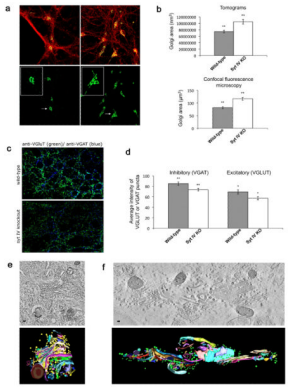

Fig. 2.

Syt IV −/− mice show an enlarged Golgi apparatus. (a) Cultured hippocampal neurons (10 DIV) were fixed and labeled with an antibody directed against the Golgi marker GM130 (green) and the synaptic vesicle protein synaptophysin (red), then imaged using laser confocal microscopy (L: wild-type. R: Syt IV −/−). Bottom panel shows only the green channel highlighting the Golgi. Inset shows a single Golgi from WT or syt IV −/− neurons. (b) Average area occupied by WT and syt IV −/− Golgi, calculated from five 250 nm tomograms (top panel; wild-type mean=7.4×10^7 nm^3, syt IV −/− mean=10.4×10^7 nm^3), or from 22 confocal image reconstructions from each genotype (bottom panel; WT mean=81.56 μm^3, syt IV −/− mean=116.75 μm^3). Error bars indicate SEM. Statistical significance was determined by a Student's *t*-test where * $P<0.05$, ** $P<0.01$, and *** $P<0.001$. (c) Cultured hippocampal neurons from syt IV −/− and WT littermates immunostained for VGluT1 and VGAT to mark excitatory and inhibitory synaptic vesicles, respectively. (d) Quantitation of intensity of VGluT1 or VGAT signal at synapses in syt IV −/− and WT cultures. VGluT and VGAT channels were thresholded separately to include all recognizable puncta, and average intensity was determined using Metamorph software ($n=9$ images from three different cultures; error bars indicate SEM; statistical significance was determined by a Student's *t*-test where * $P<0.05$, ** $P<0.01$, and *** $P<0.001$; for VGAT $P=.012$, and for VGluT $P=.026$). (e) Cultured hippocampal neurons (10 DIV) were high-pressure frozen and processed for electron tomography. A slice through a tomographic reconstruction of a WT Golgi (top), and the subsequent model (bottom). Scale bar is 40 nm. (f) A slice through a tomographic reconstruction of a syt IV −/− Golgi (top) and subsequent model (bottom). Scale bars=35 nm.

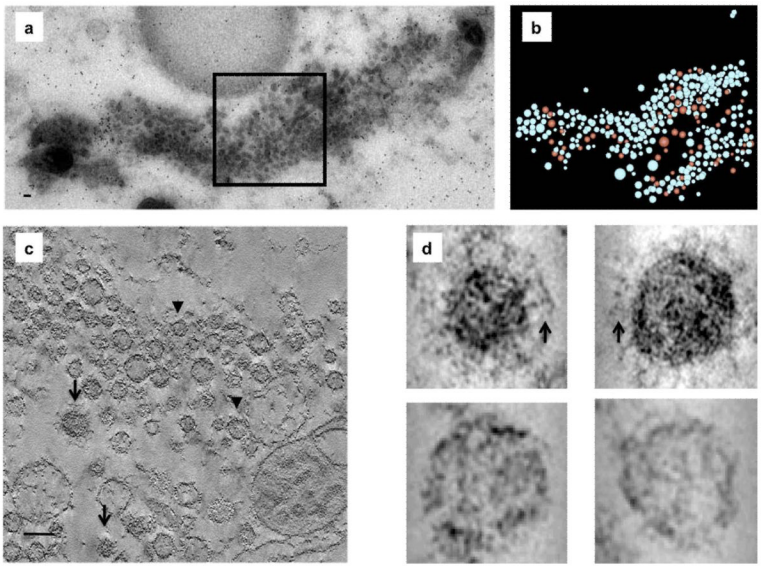

Fig. 3.

Syt IV −/− neurons have a large vesicle pool in close proximity to the Golgi. (a) Cultured hippocampal neurons (10 DIV) were high-pressure frozen and processed for electron tomography. Electron micrograph of a 250 nm slice through syt IV −/− neurons approximately 1.0 μm from the TGN showing a large vesicle pool. (b) A model of the tomographic reconstruction of the boxed region in panel A shows a mix of clear (blue) and clathrin-coated (red) vesicles. (c) Slice through a tomographic reconstruction of the boxed area in panel a. Arrows indicate clathrin-coated vesicles and arrowheads indicate clear vesicles. (d) 2×2 array of individual vesicles either with a characteristic clathrin triskilion (arrows, top row) or without (bottom row). Scale bars=35 nm.

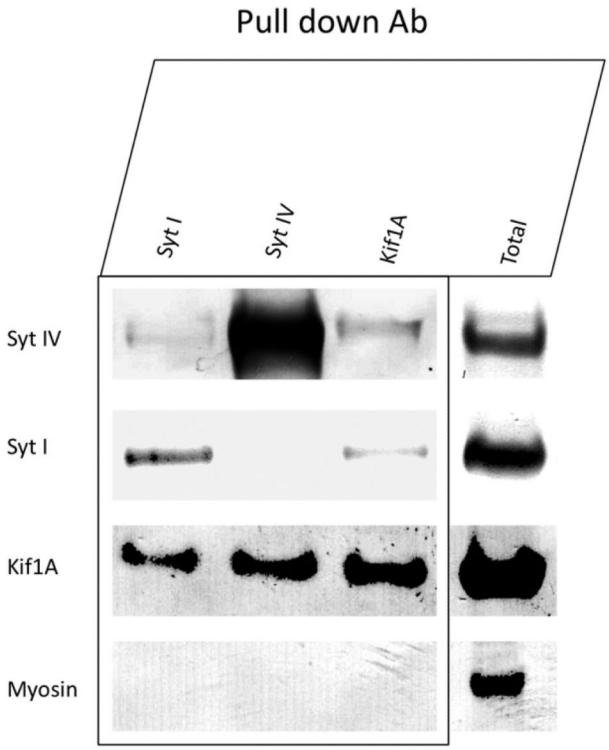

Fig. 4.

Syt IV coimmunoprecipitates with KIF1A from mouse brain. Whole mouse brains were homogenized, solubilized and incubated with either syt IV, syt I, or KIF1A primary antibodies overnight. Samples were incubated with protein A Sepharose beads for 1 h, pelleted and then analyzed by SDS-PAGE and western blot. Syt IV coimmunoprecipitates KIF1A. Similarly, KIF1A coimmunoprecipitates syt IV. Syt I coimmunoprecipitates both KIF1A and syt IV, but syt I and syt IV did not co-immunoprecipitate each other to a significant extent.